Hindawi Publishing Corporation
International Journal of Antennas and Propagation
Volume 2014, Article ID 498767, 9 pages
http://dx.doi.org/10.1155/2014/498767

*Research Article*

# A Study of the Anechoic Performance of Rice Husk-Based, Geometrically Tapered, Hollow Absorbers

**Muhammad Nadeem Iqbal,[1] Mohd. Fareq Malek,[2] Yeng Seng Lee,[1] Liyana Zahid,[2] and Muhammad Shafiq Mezan[2]**

[1] *School of Computer & Communication Engineering, Universiti Malaysia Perlis (UniMAP), Pauh Putra Campus, Arau, 02600 Perlis, Malaysia*
[2] *School of Electrical System Engineering, Universiti Malaysia Perlis (UniMAP), Pauh Putra Campus, Arau, 02600 Perlis, Malaysia*

Correspondence should be addressed to Muhammad Nadeem Iqbal; mr.nadeemiqbal@gmail.com

Received 29 August 2013; Accepted 25 November 2013; Published 5 January 2014

Academic Editor: Ananda Sanagavarapu Mohan

Copyright © 2014 Muhammad Nadeem Iqbal et al. This is an open access article distributed under the Creative Commons Attribution License, which permits unrestricted use, distribution, and reproduction in any medium, provided the original work is properly cited.

Although solid, geometrically tapered microwave absorbers are preferred due to their better performance, they are bulky and must have a thickness on the order of $\lambda$ or more. The goal of this study was to design lightweight absorbers that can reduce the electromagnetic reflections to less than −10 dB. We used a very simple approach; two waste materials, that is, rice husks and tire dust in powder form, were used to fabricate two independent samples. We measured and used their dielectric properties to determine and compare the propagation constants and quarter-wave thickness. The quarter-wave thickness for the tire dust was 3 mm less than that of the rice husk material, but we preferred the rice-husk material. This preference was based on the fact that our goal was to achieve minimum backward reflections, and the rice-husk material, with its low dielectric constant, high loss factor, large attenuation per unit length, and ease of fabrication, provided a better opportunity to achieve that goal. The performance of the absorbers was found to be better (lower) than −20 dB, and comparison of the results proved that the hollow design with 58% less weight was a good alternative to the use of solid absorbers.

## 1. Introduction

Electromagnetic interference (EMI) is a serious threat to electronics-based civil and military infrastructures [1, 2]. Various types of natural and man-made EMI sources have been identified that can lock, upset, damage, and cause malfunctions in sensitive electronic components in extremely complex and mission-critical systems [3–5]. Electronic devices must follow the electromagnetic compatibility (EMC) standards which impose certain conditions on the electronic devices before they can be marketed [6–9]. Comprehensive EMC testing of these devices is conducted to determine their emissions and susceptibility levels within specially designed, shielded, reflectionless facilities, that is, anechoic chambers. In these chambers, geometrically tapered, synthetic, carbon-impregnated foams with thicknesses on the order of $\lambda$ or greater are used [10]. These absorbers are made from flexible, polyurethane foam, which is a heterochain polymer, synthesized by the reaction of isocyanate (–NCO functional group) compounds and polyether polyol alcohol (–OH functional group) [11, 12]. Isocyanates are hazardous compounds and can cause significant respiratory problems, such as asthma and decreased lung function [12]. The main cause of these health hazards is the inhalation of the foam dust that contains traces of isocyanates and contaminated fibers.

Agricultural waste, especially rice husks, is a nonhazardous natural source of lossy carbon [13, 14] that can be used as a filler in a polymer matrix to absorb the EMI noise. Rice husks are a waste material produced by the rice milling industry, and this waste material is used along with its by-product, that is, rice husk ash, in the cement industry, power production equipment, and furnaces [15]. Rice husk material is a low-cost, low-density raw biomass material that is readily available for use in manufacturing value-added,

silicon-based products [16]. Rice-husk waste amounts to 20–25% of the harvested product [17], and its use in the production of cheaper, value-added products also reduces the environmental pollution associated with burning rice husks, which has been a common practice for many years [18].

In previous research [19–23], the main focus of the researchers was to identify the rice-husk material as a new, microwave-energy-absorbing material, develop simulation designs, and evaluate its ability to reflect electromagnetic noise. Most such research involved the use of simulation tools to investigate solid forms that were shaped as pyramids or wedges, and only a few of the studies presented experimental results indicating how well the material performed. In addition, the range of frequencies investigated was very narrow, and no data were provided concerning the hollow structures fabricated from the rice-husk material. Similarly, the extent of the attenuation of the microwave signal per unit length of the rice-husk and tire-dust material was not investigated even though it is a very important parameter that is required to determine the minimum thickness of the absorber. Obviously, hollow structures will be beneficial in reducing the overall weight of the absorbing material used within an anechoic facility.

In this study, a very simple method was used to fabricate and characterize the rice husk-based, hollow-structure, microwave absorbers. First, we measured the complex dielectric properties of the two waste materials and used these properties to determine and compare attenuation constants. Rice-husk material was preferred over the tire-dust material for the fabrication of the hollow structures because of its high loss factor and comparatively large, spatial decay rate. The hollow absorbers that we designed were investigated to determine their anechoic performance over the broad range of frequencies from 4 to 20 GHz.

## 2. Geometric Tapering of Lossy Material

*2.1. Solid Pyramidal Structure.* Physical or geometrical tapering of the lossy material is a type of broadband impedance-matching technique to minimize the reflections at the interfaces in the required pass band. In this concept, the absorber is modelled as a single structure composed of an infinite number of thin sheets (impedance transformers). However, the volume of the successive sheets increases gradually with a constant ratio from the tip of the pyramid to the bottom, as shown in Figure 1. Due to the gradual change in the volume of the material, each successive layer of the pyramidal absorbing structure exhibits different dielectric properties and characteristic impedances. According to transmission-line theory, the number of impedance transformers must be infinite to smooth the impedance discontinuities at the interfaces. Adding an infinite number of layers to the absorbing structure improves the impedance matching at the cost of large material thickness in terms of the wavelength to achieve minimum reflections at the air-absorber interface. Impedance at the $i$th interface can be found by using the information of the propagation constant ($\gamma_i$) and characteristic impedance ( $\eta_i$ and $\eta_{i+1}$) of each layer according to the transmission line theory as follows:

$$Z_i = \eta_i \frac{\eta_{i+1} + \eta_i \tanh(\gamma_i d_i)}{\eta_i + \eta_{i+1} \tanh(\gamma_i d_i)}. \tag{1}$$

*2.2. Hollow Pyramidal Structure.* Hollow pyramidal absorber can be considered as a diverging structure having an infinite number of square loops (apertures). The area of each successive square loop is greater than the preceding loop. Above-mentioned theory Section 2.1 is valid only for the thick lossy material (solid absorbers), which can be modeled as an infinite-section transmission line. In case of a hollow pyramidal structure, the minimum reflections at the boundaries do not guarantee the attenuation of the signal within the absorbing pyramid without considering the loss per unit thickness of the walls of the absorbing pyramid. Hence, the walls of a hollow pyramidal absorber must be lossy so that the incident EM energy can be dissipated into heat by the Joule heating principle without reflections [7].

The propagation characteristics of the incident EM signal through the lossy medium ($\sigma_{\text{eff}} = \sigma + \omega\varepsilon'' \neq 0$) usually are described by the wave propagation constant, $\gamma = \sqrt{j\omega(\sigma_{\text{eff}} + j\omega\varepsilon')} = \alpha + j\beta$, where $\alpha$(NP/m) and $\beta$(rad/m) are the attenuation and phase constants, respectively, of the wave propagating through the lossy medium. The exact equations for these two constants are expressed as [24, 25]

$$\alpha = \omega\sqrt{\mu\varepsilon'}\left\{\frac{1}{2}\left[\sqrt{1+\left(\frac{\sigma_{\text{eff}}}{\omega\varepsilon'}\right)^2} - 1\right]\right\}^{1/2},$$
$$\beta = \omega\sqrt{\mu\varepsilon'}\left\{\frac{1}{2}\left[\sqrt{1+\left(\frac{\sigma_{\text{eff}}}{\omega\varepsilon'}\right)^2} + 1\right]\right\}^{1/2}; \tag{2}$$

here, $\mu$, $\varepsilon'$, and $\sigma_{\text{eff}}$ are the complex magnetic permeability, real part of complex permittivity, and effective conductivity of the lossy medium.

*2.3. Metal-Backed Layer of a Lossy Material .* A single layer of a metal-backed lossy material (effective in suppressing the low frequency signals) can be modeled as a short-circuited transmission line. In this case, we can transform (1) as, $Z_i = \eta_i \tanh(\gamma_i d_i)$ and the reflection loss can be calculated by using the following equation to evaluate the anechoic performance:

$$\text{RL (dB)} = 20 \log \left| \frac{Z_i - Z_0}{Z_i + Z_0} \right|. \tag{3}$$

To achieve the best anechoic performance (less echoes), it is clear that it is very important to know the propagation characteristics within the lossy material.

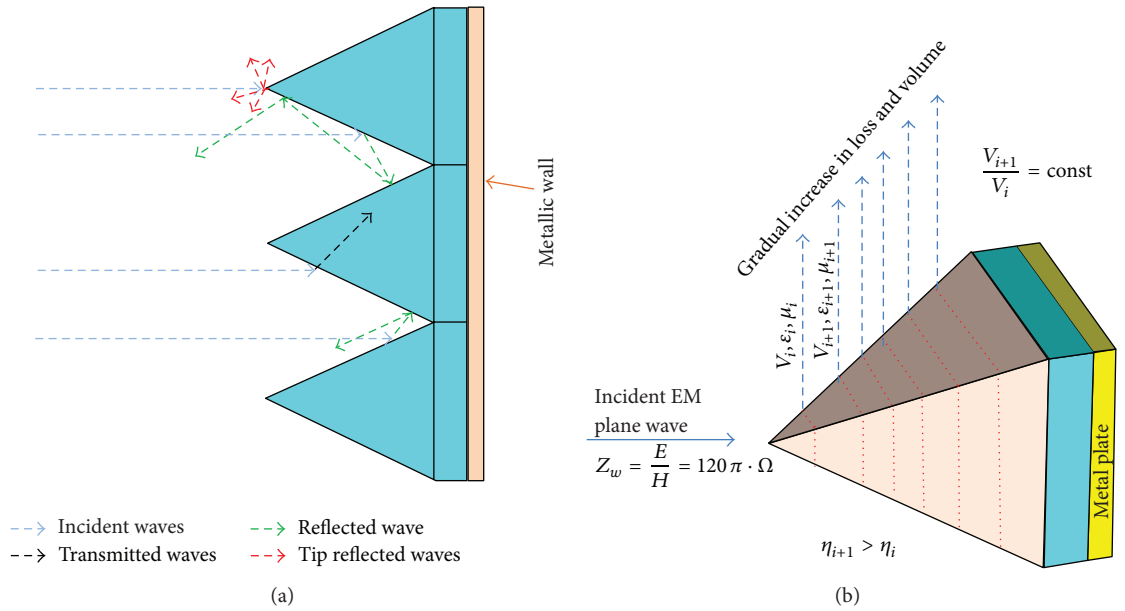


FIGURE 1: Illustration of wave-absorber interactions: (a) possible interactions of incident EMI signal with the wall of the anechoic chamber that is lined with a periodic array of pyramids; (b) sketch of a unit cell of the array of solid pyramids, showing a gradual increase in volume and loss factor along the axis of the wave propagation.

## 3. Research Methodology

*3.1. Sample Fabrication and Characterization Method.* Two independent samples were fabricated by using simple, laboratory-scale methods, as described in [22]. In one of the samples, we mixed the rice husks (54.3% by weight) with unsaturated polyester resin UPR (43.4% by weight) and methyl ethyl ketone peroxide MEKP (2.3% by weight). In the second sample, we used tire dust (70% by weight) with UPR (28% by weight) and MEKP (2% by weight). We used UPR as a polymer matrix to bind the fillers, that is, rice husks and tire dust, and MEKP was used as a catalyst to cure the UPR.

In this study, we used an open-ended, coaxial probe (Figure 2(a)) to measure the dielectric properties of the fabricated samples. This method provided broadband, nondestructive, rapid experimental means to measure both components of complex permittivity [27–29]. We performed a "three standard" calibration of the probe before beginning the measurements, and water, air, and a load, which are shown in Figure 2(b), were used as calibration standards. Figure 2(c) shows a typical experimental setup for the measurement of the dielectric properties in the frequency range of 4–20 GHz. The apparatus used for the dielectric characterization in this study included the Agilent 85070B High-Temperature Dielectric Probe, Agilent Vector Network Analyzer, and Agilent 85070 software. The measurement procedure is very simple and easy; the end of the probe is brought into the contact with the flat surface of the sample, and the probe senses the signal that is reflected from the sample [30]. Then, this reflected signal is displayed on the network analyzer by using the software.

*3.2. Frequency Spectrum of Dielectric Properties.* Figure 3 shows the frequency spectrum of the relative complex permittivity ($\varepsilon_r = \varepsilon_r' - j\varepsilon_r''$) for the two samples composed of two wastes. The measured values of the real part of the relative complex permittivity for the two samples are greater than that for air, which shows their ability to be polarized to a greater extent than air. The overall pattern of the real part ($\varepsilon_r'$) decreased in values as the frequency increased. The overall dielectric constant for the tire-dust sample for the entire frequency spectrum (4–20 GHz) was in the range of 3.06–4.50, which was greater than the range for the rice-husk material (1.75–2.80). This was due to the presence of the high dielectric constant material, that is, rubber, which is the major component in the tire dust. The results showed fluctuations (ripples), and the deviations of the amplitudes of these ripples were within the range of 0.11–0.60.

These fluctuations were due to the nonuniform nature of the material and also to the presence of discontinuities in the impedance, which caused reflections at the interface of the probe and the samples at high frequencies. In addition, it also can be seen in Figure 3 that the low-frequency regime

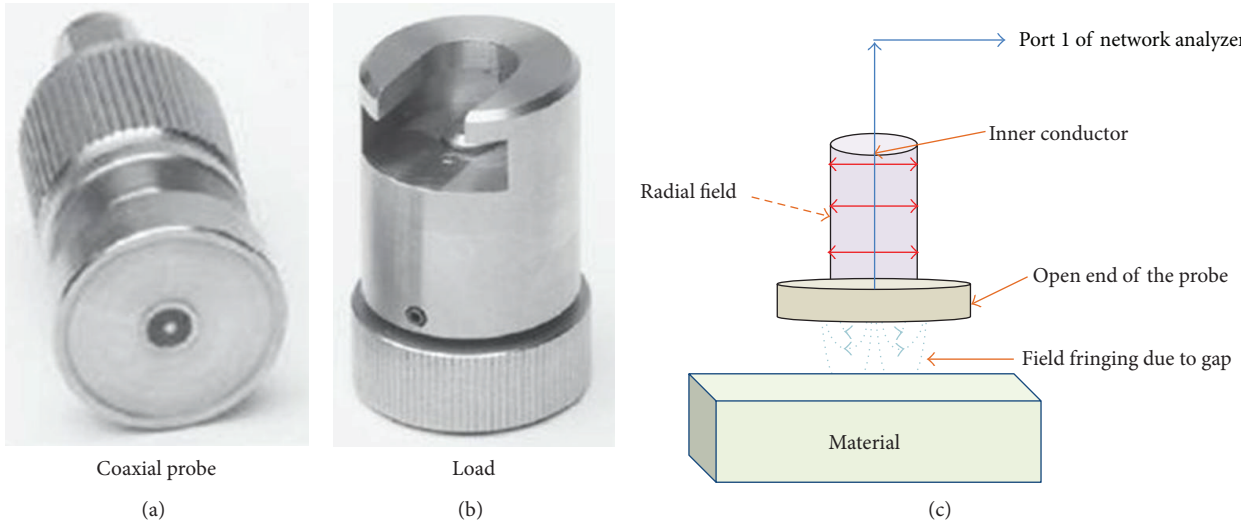


FIGURE 2: Equipment and setup for the measurement of dielectric properties of the two samples. (a) Cylindrical, open-ended, and coaxial probe [26]. (b) Load for the calibration of the open-ended probe [26]. (c) Schematics of the experimental setup, showing field infringement at the open end of the probe due to abrupt change in impedance.

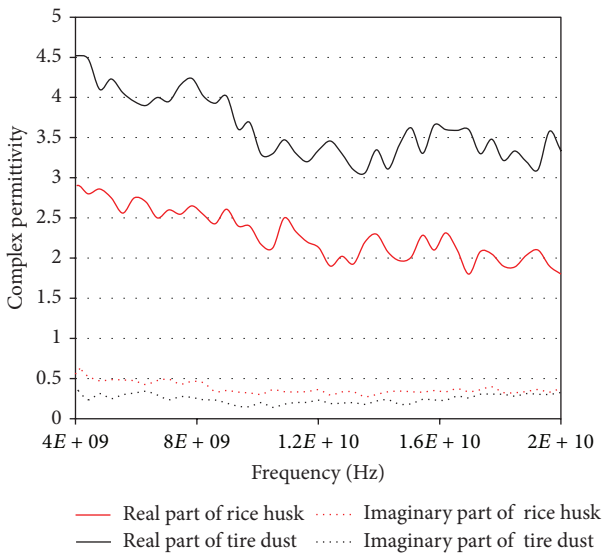


FIGURE 3: Frequency spectrum of the complex permittivity of the two samples fabricated using rice husks and tire dust.

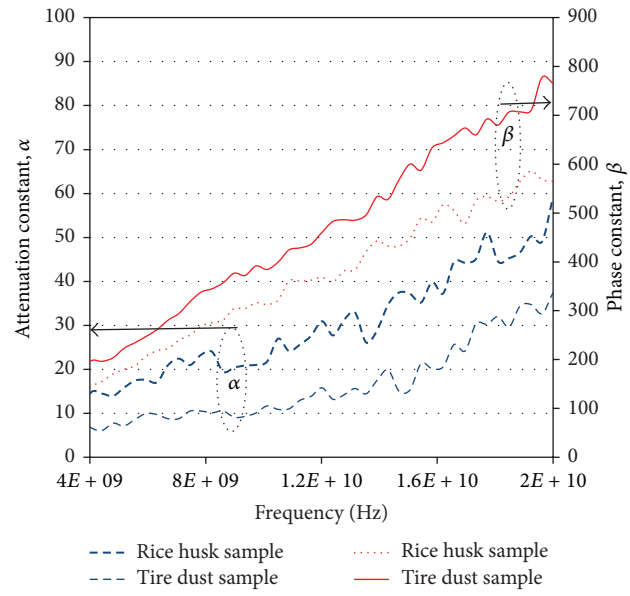


FIGURE 4: Frequency spectrum of the propagation constants of the two samples, that is, rice husks and tire dust based on their measured dielectric properties.

(4–8 GHz) has smaller fluctuations than the high-frequency regime. At high frequencies, the dimensions of the gap (air pocket), which is formed due to the lose contact between the surface of the sample and the flat end of the probe, become a very critical issue because it is much easier for small wavelength signals to leak from the small gaps compared to large wavelength signals. Figure 3 also shows that the sample composed of rice husks had the greatest loss factor (ranging from 0.30 to 0.60), whereas the sample composed of tire dust had the smallest values of loss factor (0.18 to 0.40). A detailed comparison of the measured complex dielectric properties that were measured up to two decimal places in multiple frequency bands is presented in the Table 1.

*3.3. Attenuation Constant and Quarter-Wave Thickness of the Two Waste Materials.* In considering microwave absorption, the imaginary part ($\varepsilon_r''$) is the most important of the dielectric properties, because it has a direct relation with the dissipation of the microwave energy within the material. However, the dielectric storage capability of the medium, that

Table 1: Measured range of dielectric properties of the two fabricated samples in different frequency bands.

| Sample | Properties | C-band (4–8 GHz) | X-band (8–12 GHz) | $K_u$-band (12–18 GHz) |
|---|---|---|---|---|
| Rice husk | $\varepsilon_r'$ | 2.50–2.80 | 2.00–2.60 | 1.75–2.25 |
| | $\varepsilon_r''$ | 0.45–0.60 | 0.30–0.48 | 0.30–0.40 |
| Tire dust | $\varepsilon_r'$ | 3.90–4.50 | 3.25–3.90 | 3.06–3.60 |
| | $\varepsilon_r''$ | 0.25–0.40 | 0.17–0.25 | 0.17–0.30 |

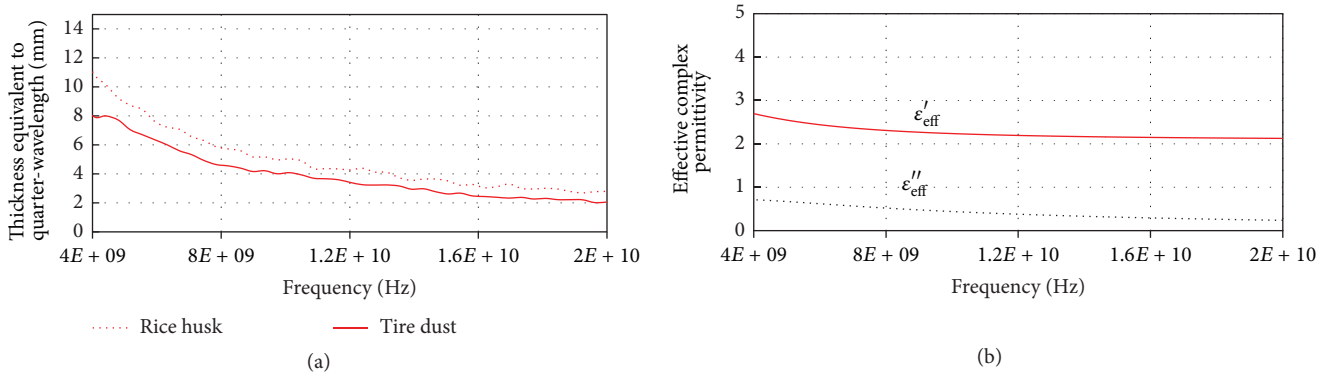


Figure 5: (a) Thickness equivalent to the quarter-wavelength based on the measured dielectric properties for rice-husk and rubber tire-dust material. (b) Calculated effective dielectric properties for hollow pyramidal absorber for wall thickness of 10 mm and fill factor $g = 0.32$.

is, its capacitance, affects the speed at which the signal is propagated. Figure 4 shows the propagation parameters, that is, attenuation ($\alpha$) and phase constant ($\beta$), based on the measured dielectric properties ($\varepsilon_r'$ and $\varepsilon_r''$) for the rice-husk and tire-dust materials. All the results show resonances at high frequencies, but the resonances in case of $\alpha$ are more prominent than those in the case of $\beta$. This occurs because $\alpha$ has a strong dependence on the loss factor, $\varepsilon_r''$. There are many factors that can affect the loss factor $\varepsilon_r''$ of the pyramidal-shaped, composite material, but the most important factor is the inhomogeneous mixing of the chemical constituents. If we ignore these resonances for the sake of analysis, it is clear that the two parameters, $\alpha$ and $\beta$, have overall positive slopes, that is, $\alpha'(f) > 0$ and $\beta'(f) > 0$, and they increase continually as frequency increases. However, the values for the attenuation constant of the tire dust are smaller than those for the rice husk, which confirms that the rice-husk material is lossier than the tire-dust material. This behavior is due to the frequency dependence (dispersion) of the constitutive parameters ($\sigma_{\text{eff}}, \varepsilon_r', \varepsilon_r''$) of the two materials. Tire dust has a low dielectric loss factor and a high dielectric constant, which explains the fact that its attenuation per unit length is smaller than that of the rice husks. The phase constant ($\beta$) values for the tire-dust material were greater than those for the rice-husk material over the entire frequency range because of the high dielectric constant of the tire dust.

The higher value of the dielectric constant of the tire dust indicated that the signal was propagated at a slow speed due to the large refractive index of the medium. This shows that the wavelength of the transmitted wave inside the tire-dust material decreases more rapidly than that of the rice-husk material; hence the thickness equivalent to the quarter wavelength ($\lambda/4$) of the wave is less for the tire-dust material. Figure 5 shows the decrease in the thickness equivalent to the quarter-wavelength of the two materials with increase in the frequency. The maximum thickness of the tire-dust material, equivalent to the quarter-wavelength at the lowest $\beta = 197$ NP/m, is 11 mm for the lowest operating frequency of 4 GHz, whereas the rice-husk material required 11 mm at 4 GHz for its lowest $\beta = 142$ NP/m.

However, for the same thickness of the two materials, the attenuation of the amplitude of the wave per unit length for tire-dust is less than that of the rice husk material. We preferred the rice-husk material for the fabrication of the hollow, pyramidal, microwave absorbers on the basis of its higher loss factor and attenuation per unit length, which make it possible to attenuate microwave energy within a thin layer.

Effective dielectric properties for the hollow absorber for wall thickness of 10 mm are also shown in Figure 5(b). These values were calculated by using the actual bulk dielectric properties (Figure 3) and fraction of the volume (fill factor) occupied by the rice husk material in hollow pyramid according to [31]. However, it has been mentioned in [31] that effective layer model is adequate only for $p < \lambda$, where $p$ is the period of the periodic structure. We were interested to design a lightweight and broadband small absorber; hence a value of $p = 50$ mm was preferred on the basis of our previous study for solid pyramid design [20].

*3.4. Determination of Optimum Wall Thickness.* We performed a parametric study by using commercially available CST Microwave Studio software to determine the optimum

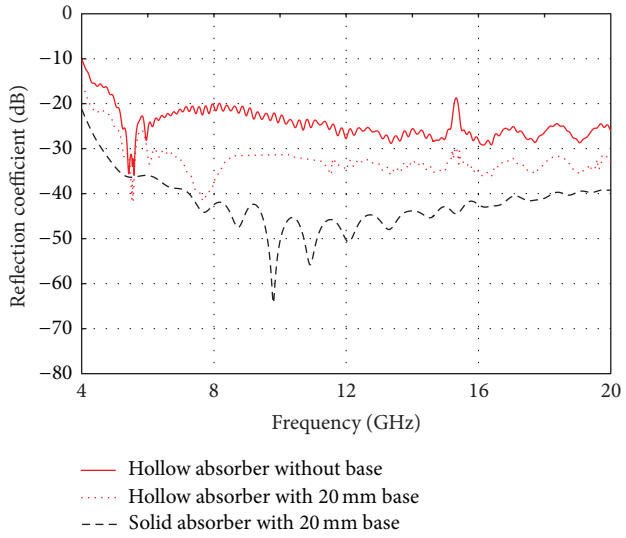


FIGURE 6: Reflection coefficient as a function of frequency for 10 mm thick-walled hollow (with and without base part) and a solid pyramidal absorber.

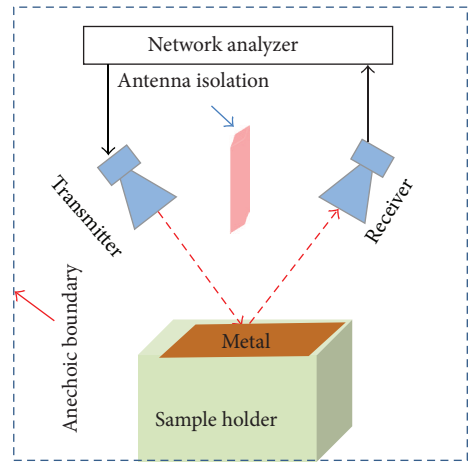


FIGURE 7: Schematics of the setup for the measurement of reflection coefficient of metal plate using the S21 parameter.

FIGURE 8: Fabricated hollow pyramidal parts of the absorbers, without a square base part, height (11 cm), and average wall thickness of 10 mm.

value of the wall thickness for the hollow absorber. Figure 6 shows the values of reflection coefficients for the pyramidal hollow absorber (with and without a 20 mm thick and 50 mm×50 mm square base part composed of rice husks) and a solid pyramidal absorber. In all three cases absorbers were backed by a perfect electric conductor (PEC). The optimum value of the wall thickness was found to be 10 mm for which better (lower) than −10 dB results were achieved for the absorber without square base part. It can be seen that the overall performance is better (lower) than the −20 dB in the frequency spectrum of 5 to 20 GHz. Figure 6 also shows that −20 dB and −25 dB performances started at 4.2 GHz and 5 GHz, respectively, with the insertion of base part. Best performance was seen for the case of solid absorber and it had shown better (lower) than −30 dB and −40 dB performances at 5 GHz and 7.2 GHz, respectively. However, in this case the weight of the absorber was 138% more than the 10 mm thick-walled hollow pyramidal absorber.

## 4. Measurement of Anechoic performance of Hollow Absorbers

*4.1. Method for Reflectivity Measurements.* Anechoic performance of the hollow absorbers was evaluated in terms of their reflectivity. We measured the bistatic reflectivity of hollow pyramidal absorbers by using a very simple, two-antenna, free-space reflectivity measurement method, also known as the contactless, nondestructive, evaluation method [32–34]. The first step was the calibration of the Agilent PNA 8362B Network Analyzer (NA) by using calibration standards, that is, the short open load through (SOLT) calibration technique. The time-gating technique also was used to eliminate or "gate out" unwanted multiple reflections, that is, reflections from the transmitter, receiver, and supporting structures. Next, we measured the reflection coefficient of the metal plate without the absorber and with the absorber, that is, $S_{21,\text{metal}}$ and $S_{21,\text{absorber}}$, respectively, according to the setup shown in Figure 7.

The bistatic reflectivity was measured by comparing the two reflection coefficients in "dB" units. We used the metal plate at the back of the absorber and assumed that there would be no transmission through the metal plate, that is, $T(\omega) = 0$, throughout the spectrum of frequencies that was investigated [35]. With this assumption, the reflectivity of the absorber was related to the absorption within the absorber as $A(\omega) = 1 - R(\omega)$, which shows that the absorber's minimum reflectivity occurred at maximum absorption and vice versa [35].

Figure 8 shows the hollow absorbers that were fabricated. We chose to make the hollow pyramids with a height of 11 cm, which was greater than one wavelength at the lowest working frequency (4 GHz). We fabricated the hollow structures in an array of 3 × 3 pyramids, with a periodicity of 5 cm, which was greater than the half wavelength at the lowest frequency. The thickness of the walls of the pyramids was equivalent to one quarter of the wavelength (10 mm) at the lowest frequency; this was based on the results of Sections 3.3 and 3.4. In case of

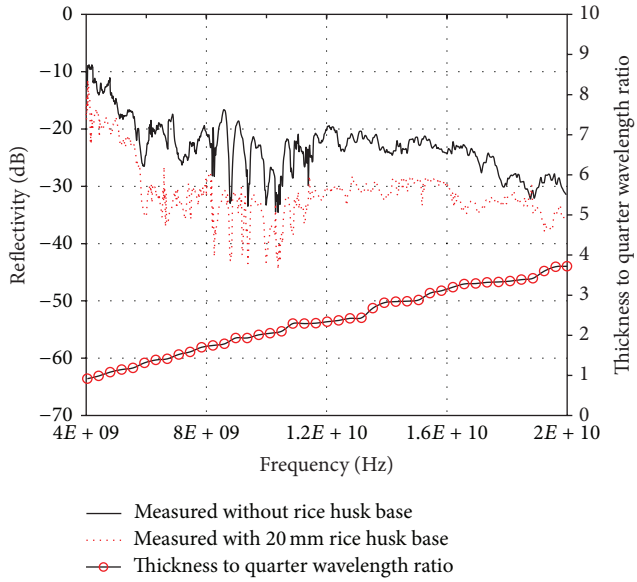


Figure 9: Measured bistatic, normal reflectivity performance of the hollow pyramids with reference to a metal plate along with the thickness-to-quarter- wavelength ratio based on the actual dielectric properties.

10 mm thickness, total weight of a unit cell (hollow pyramid) was 42% of the solid pyramid, that is, 58% less weight.

*4.2. Frequency Spectrum of Bistatic Reflectivity Measurements.* Figure 9 shows the measured bistatic, reflectivity performances of the fabricated, hollow structures for a normal incidence angle when the electric and magnetic field vectors were transverse to the periodic structure.

In addition, the measured normal reflectivity (relative to a metal plate) of the rice husk-based, hollow absorber was less than −10 dB in the frequency range of 4 to 20 GHz. Results improved with the insertion of base part between hollow pyramid and PEC back plate and lower than −20 dB and −30 dB performances started at 5 GHZ and 6 GHZ, respectively. The overall behaviors of the simulated (Figure 6) and measured (Figure 9) reflectivity curves show good agreement.

Large resonances were observed in the frequency range of 5.7 GHz to 12 GHz. The resonances exhibited maximum variations in the frequency range of 8 GHz to 11 GHz. These resonances occurred in the frequency range for which the ratio of thickness to the length of the quarter wave was <2.5. When a rice husk-based, flat, 20 mm thick sheet was inserted between the hollow pyramids and the metal plate, a decrease of −5 dB to −10 dB in reflectivity was observed in the frequency range that was investigated, which is a more practical situation.

Figure 9 also shows a decrease in the reflectivity (more absorption) as the ratio of the absorber's thickness to the length of the quarter wave increased. Reflectivity performance of −10 dB to −15 dB was observed in a half portion of the C-band, when the thickness-to-quarter-wave length ratio was less than the 1.5 for the case of no base plate. The results

Figure 10: Propagation of crack due to the effect of high contents (greater than 70%) of the rice-husks on the structural stability of the rice husk-UPR composite.

exhibited a further improvement in the normal reflectivity (−20 dB to −31 dB) in X-band up to 11 GHz. However, this improvement in reflectivity was observed when thickness-to-quarter-wave length ratio was 1.5–2.5. However, this portion of the spectrum for which the thickness-to-quarter-wave length ratio was less than 2.5 showed resonances, which were due to the fact that greater thickness is required to absorb low-frequency microwaves properly within the lossy medium. The lossy medium becomes transparent to low-frequency microwaves when the thickness-to-quarter-wave length ratio is very small. At high frequencies, the medium acts as a resistive medium and microwave energy is converted to heat when the thickness-to-quarter-wave length ratio increases.

*4.3. Sample Drop Test.* Hollow absorbers were fabricated in composite form and composed of rice-husks (as lossy filler) and unsaturated polyester resin (UPR) as a matrix. In order to check the vulnerability of each sample we dropped pyramids one by one from a height of 1 m. In our study, we observed that the pyramids with high contents of rice-husks were more vulnerable than the samples with high resin contents. Additionally, the most vulnerable point was found to be the tip of each pyramid where bulk of the material was the least (also shown in Figure 8). In worst case, the dimensions of the damaged tips were found to be less than 3 × 3 mm. However, we used the rice-husks as a filler to provide the lossy medium in the UPR polymer matrix, so high contents of resin will affect the wave attenuation characteristics of the absorber. The optimum weight fraction of rice-husks was found to be 35 to 45%, of the overall composite, for which least structural damage was observed. Figure 10 shows the effect of high (greater than 70%) contents of rice-husks on the flat 10 mm thick composite within one week after the fabrication. Propagation of cracks is visible which indicates the weak bonding of the constituents. We selected 40% weight fraction of the rice-husks for the fabrication of hollow absorbers. Additionally, we truncated the tips in order to simulate the actual worst case (damaged-tip) scenario and performance was evaluated. It was observed that the overall measured results remained the same for both of the cases, that is, before and after the drop test. However, we also performed

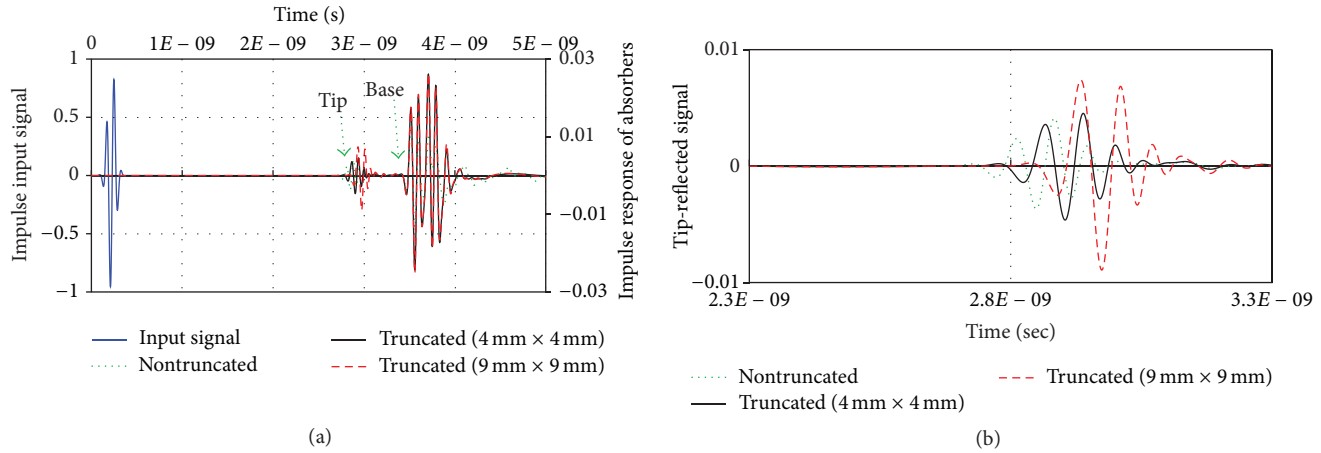


Figure 11: Time domain wave-absorber interaction and effect of truncated tips. (a) Overall impulse response of the wave-absorber system; (b) signals that were reflected from the tips.

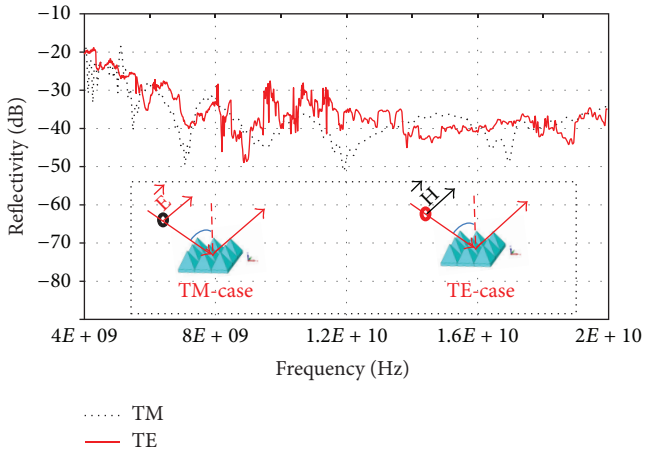


Figure 12: Oblique angle reflectivity performance of the rice husk-based, hollow pyramidal structures in TM and TE polarization at 45° incident angle.

simulations for the absorbers with different truncated tips and time domain results are presented in Figure 11.

It can be observed that the amplitude of the signal that was reflected from the 4 × 4 mm truncated tips had similar response (with a small time delay) to the nontruncated case. Signal that was reflected from the 9×9 mm truncated tips had shown the largest amplitude due to the abrupt change in the dielectric properties of the medium. Delay in the time of arrivals of the signals which were reflected from the truncated tips is due to the extra distance the incident wave had travelled. Dielectric properties vary smoothly from tips to the interior of the nontruncated, pyramidal absorbers and results in smaller reflections (less impedance discontinuities) at the tips.

*4.4. Sample Rotation and Oblique Angle Reflectivity Spectrum.* The hollow, microwave-absorbing structure was periodic and was composed of the same material (rice husks), so, ideally, its performance should be independent of the rotation of the sample. Even so, the possibility of impedance discontinuities due to the manual mixing of the constituents cannot be ignored, so the sample was rotated 360° on its axis in four steps of 90° each, and reflectivity was measured. It was observed that the sample rotation had little effect on the overall reflectivity performance. We also measured the oblique angle reflectivity performance in the range of 10° to 60° of incidence angles in transverse magnetic (TM) and transverse electric (TE) polarizations. However, the effects of edge diffractions were observed for the incident angles $\theta >$ 50°, due to the overall small dimensions of the sample. Therefore, the reflectivity performance of the hollow, microwave-absorbing structures at an oblique angle of 45° for both of the polarizations is presented in Figure 12.

It can be observed that the designed absorber has better (lower than −20 dB) performance for both of the polarizations (TE and TM).

## 5. Conclusions

The results of this experimental study led us to conclude that thin-walled, hollow structures fabricated by using rice husks in pyramidal shapes can be used efficiently to suppress the reflections caused by the wall of the anechoic chamber. The comparison of the rice husks and another waste material, that is, tire dust, showed that the rice husks were more lossier and provided more microwave attenuation per unit length than the tire dust. The results also showed that this type of innovative absorber design is equally efficient for suppressing normal and off normal (up to $\theta = 45°$) incident signals in TE and TM modes of polarization. The results also confirmed that the rice husk-based, hollow, pyramidal design fulfilled the minimum absorption criterion (−10 dB) for shielded, EMC anechoic chambers according to the MIL-STD-461F at high frequencies. This design provided good microwave absorbing characteristics, that is, <−20 dB starting from 4 GHz, with 58% less weight and material consumption

than a solid absorber. However, the compatibility of the rice-husk material with thermoplastics and flexible, high yield-strain elastic polymers still must be explored for the fabrication of flexible and durable microwave absorbers.

## Conflict of Interests

The authors declare that there is no conflict of interests regarding the publication of this paper.

## References


[1] R. Schmitt, *Electromagnetics Explained: A Handbook for Wireless/RF, EMC, and High-Speed Electronics*, Elsevier Science, Burlington, Mass, USA, 2002.

[2] J. W. Gooch and J. K. Daher, *Electromagnetic Shielding and Corrosion Protection For Aerospace Vehicles*, Springer, New York, NY, USA, 2007.

[3] T. Williams, *EMC for Product Designers*, Newness, 3rd edition, 2001.

[4] M. Glenewinkel, "System design and layout techniques for noise reduction in MCU-based systems," AN1259/D, Motorola, 1995.

[5] S. Ghosh and A. Chakrabarty, "Performance analysis of emi sensor in different test sites with different wave impedances," *Progress in Electromagnetics Research*, vol. 62, pp. 127–142, 2006.

[6] L. H. Hemming, *Electromagnetic Anechoic Chambers A Fundamental Design and Specification Guide*, Wiley-IEEE Press, New York, NY, USA, 2002.

[7] X. C. Tong, *Advanced Materials and Design For Electromagnetic Interference Shielding*, CRC & Taylor & Francis, Boca Raton, Fla, USA, 2009.

[8] D. Morgan, *A Handbook for EMC Testing and Measurement*, Peter Peregrinus, London, UK, 1994.

[9] H. W. Ott, *Electromagnetic Compatibility Engineering*, John Wiley & Sons, Hoboken, NJ, USA, 2009.

[10] S. Gu, J. P. Barrett, T. H. Hand, B.-I. Popa, and S. A. Cummer, "A broadband low-reflection metamaterial absorber," *Journal of Applied Physics*, vol. 108, no. 6, Article ID 064913, 2010.

[11] M. Ionescu, *Chemistry & Technology of Polyols for Polyurethanes*, Rapra Technology limited, Shropshire, UK, 2005.

[12] D. Klempner and V. Sendijarevic, *Polymeric Foams and Foam Technology*, Hanser, Munich, Germany, 2nd edition, 2004.

[13] D. S. Prasad and A. R. Krishna, "Fabrication and characterization of a356. 2-rice husk ash composite using stir casting technique," *International Journal of Engineering Science*, vol. 2, no. 12, pp. 7603–7608, 2010.

[14] C. R. T. Tarley and M. A. Z. Arruda, "Biosorption of heavy metals using rice milling by-products. Characterisation and application for removal of metals from aqueous effluents," *Chemosphere*, vol. 54, no. 7, pp. 987–995, 2004.

[15] K. Kartini, H. B. Mahmud, and M. S. Hamidah, "Absorption and permeability performance of selangor rice husk ash blended grade 30 concrete," *Journal of Engineering Science and Technology*, vol. 5, no. 1, pp. 1–16, 2010.

[16] S. Turmanova, S. Genieva, and L. Vlaev, "Obtaining some polymer composites filled with rice husks ash-a review," *International Journal of Chemistry*, vol. 4, no. 4, pp. 1916–9701, 2012.

[17] L. Xiong, K. Saito, E. H. Sekiya, P. Sujaridworakun, and S. Wada, "Influence of impurity ions on rice husk combustion," *Journal of Metals, Materials and Minerals*, vol. 19, no. 2, pp. 73–77, 2009.

[18] H.-S. Yang, H.-J. Kim, J. Son, H.-J. Park, B.-J. Lee, and T.-S. Hwang, "Rice-husk flour filled polypropylene composites; mechanical and morphological study," *Composite Structures*, vol. 63, no. 3-4, pp. 305–312, 2004.

[19] H. Nornikman, P. J. Soh, A. A. H. Azremi, F. H. Wee, and M. F. Malek, "Investigation of an agricultural waste as an alternative material for microwave absorbers," in *Proceedings of the Progress in Electromagnetics Research Symposium*, Moscow, Russia,, August 2009.

[20] H. Nornikman, F. Malek, P. J. Soh, A. A. H. Azremi, F. H. Wee, and A. Hasnain, "Parametric studies of the pyramidal microwave absorber using rice husk," *Progress in Electromagnetics Research*, vol. 104, pp. 145–166, 2010.

[21] H. Nornikman, F. Malek, P. J. Soh et al., "Setup and results of pyramidal microwave absorbers using rice husks," *Progress in Electromagnetics Research*, vol. 111, pp. 141–161, 2011.

[22] F. Malek, E. M. Cheng, O. Nadiah et al., "Rubber tire dust-rice husk pyramidal microwave absorber," *Progress in Electromagnetics Research*, vol. 117, pp. 449–477, 2011.

[23] H. Nornikman, P. J. Soh, A. A. H. Azremi, F. H. Wee, and M. F. Malek, "Investigation of an agricultural waste as an alternative material for microwave absorbers," *PIERS Online*, vol. 5, no. 6, 2009.

[24] C. A. Balanis, *Advanced Engineering Electromagnetics*, John Wiley & Sons, Hoboken, NJ, USA, 1998.

[25] K. Kishor, *Antenna and Wave Propagation*, I.K. Publishing House, 2009.

[26] Agilent, "Basics of Measuring the Dielectric Properties of Materials," Application Note, Printed in USA, June 2006.

[27] U. C. Hasar and O. Simsek, "An accurate complex permittivity method for thin dielectric materials," *Progress in Electromagnetics Research*, vol. 91, pp. 123–138, 2009.

[28] J. S. Bobowski, T. Johnson, and C. Eskicioglu, "Permittivity of waste-activated sludge by an open-ended coaxial line," *Progress in Electromagnetics Research Letters*, vol. 29, pp. 139–149, 2012.

[29] J. Baker-Jarvis, M. D. Janezic, P. D. Domich, and R. G. Geyer, "Analysis of an open-ended coaxial probe with lift-off for nondestructive testing," *IEEE Transactions on Instrumentation and Measurement*, vol. 43, no. 5, pp. 711–718, 1994.

[30] L. D. C. Folgueras, M. A. Alves, and M. C. Rezende, "Microwave absorbing paints and sheets based on carbonyl iron and polyaniline: measurement and simulation of their properties," *Journal of Aerospace Technology and Management*, vol. 2, no. 1, pp. 63–70, 2010.

[31] M. Johansson, C. L. Holloway, and E. F. Kuester, "Effective electromagnetic properties of honeycomb composites, and hollow-pyramidal and alternating-wedge absorbers," *IEEE Transactions on Antennas and Propagation*, vol. 53, no. 2, pp. 728–736, 2005.

[32] G. L. Friedsam and E. M. Biebl, "A broadband free-space dielectric properties measurement system at millimeter wavelengths," *IEEE Transactions on Instrumentation and Measurement*, vol. 46, no. 2, pp. 515–518, 1997.

[33] M. S. Venkatesh and G. S. V. Raghavan, "An overview of dielectric properties measuring techniques," *Canadian Biosystems Engineering*, vol. 47, pp. 15–30, 2005.

[34] Y. Zhang and Y. Ogura, "Density-independent high moisture content measurement using phase shifts at two microwave frequencies," *Journal of Microwave Power and Electromagnetic Energy*, vol. 44, no. 3, pp. 163–167, 2010.

[35] M.-H. Li, H.-L. Yang, X.-W. Hou, Y. Tian, and D.-Y. Hou, "Perfect metamaterial absorber with dual bands," *Progress in Electromagnetics Research*, vol. 108, pp. 37–49, 2010.



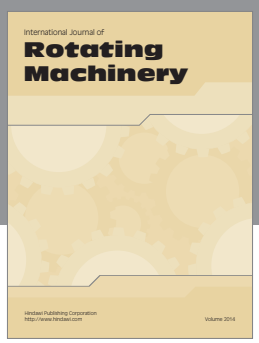




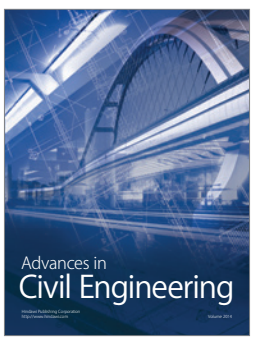


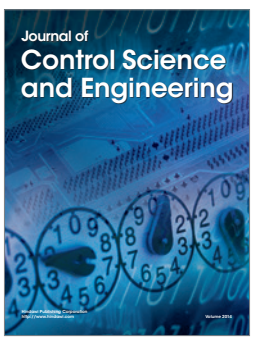



Hindawi
Submit your manuscripts at
http://www.hindawi.com